mathematics

MDPI

Article

Modelling Predator–Prey Interactions: A Trade-Off between Seasonality and Wind Speed

Dipesh Barman and Ranjit Kumar Upadhyay *

Department of Mathematics & Computing, Indian Institute of Technology (Indian School of Mines), Dhanbad 826004, India; dipeshrs2018@gmail.com
* Correspondence: ranjit@iitism.ac.in

Abstract: Predator–prey interactions do not solely depend on biotic factors: rather, they depend on many other abiotic factors also. One such abiotic factor is wind speed, which can crucially change the predation efficiency of the predator population. In this article, the impact of wind speed along with seasonality on various parameters has been investigated. Here, we present two continuous-time models with specialist and generalist type predators incorporating the effect of wind and the seasonality on the model parameters. It has been observed that wind speed plays a significant role in controlling the system dynamics for both systems. It makes the systems stable for both of the seasonally unperturbed systems. However, it controls the chaotic dynamics that occur in case of no wind for the seasonally perturbed system with the predator as a specialist. On the other hand, for the seasonally perturbed system with a generalist predator, it controls period-four oscillations (which occur considering no wind speed) to simple limit-cycle oscillations. Furthermore, the wind parameter has a huge impact on the survival of predator species. The survival of predator species may be achieved by ensuring a suitable range of wind speeds in the ecosystem. Therefore, we observe that seasonality introduces chaos, but wind reduces it. These results may be very useful for adopting necessary management for the conservation of endangered species that are massively affected by wind speed in an ecosystem.

Keywords: predator–prey interactions; wind effect; chaos; Hopf bifurcation; period-four oscillation; limit cycle

MSC: 92B05; 92D40; 92D25; 34D20

Citation: Barman, D.; Upadhyay, R.K. Modelling Predator–Prey Interactions: A Trade-Off between Seasonality and Wind Speed. *Mathematics* **2023**, *11*, 4863. https://doi.org/10.3390/math11234863

Academic Editor: Giancarlo Consolo

Received: 15 September 2023
Revised: 30 November 2023
Accepted: 1 December 2023
Published: 4 December 2023

1. Introduction

Mathematical ecology is an inter-disciplinary field that studies various ecological phenomena with the help of mathematical modelling to understand how a small change to environmental parameters affects the system's characteristic. The study of predator–prey interactions by using mathematical modelling becomes very useful in different contexts such as saving endangered species, controlling disease outbreak, etc. One well-known viewpoint is that studies of such types of mathematical models have been mainly based on biotic factors and direct effects. However, as of late, numerous scientists have given a lot of consideration to investigate the job of backhanded impacts: for example, predator-prompted dread impact in system dynamics [1–3]. However, abiotic factors such as temperature, climate change, speed of wind, etc., may affect the interactions among different species. In the field of theoretical ecology, a sufficient number of studies have been performed in this context, but in mathematical ecology, less attention has been paid paid. Some research has been performed by considering temperature as an abiotic factor [4]. However, this leaves a knowledge deficit about how other abiotic elements affect the interactions among ecological communities. Investigation on the effects of climate change all over the globe has recently received renewed interest from theoretical ecologists, particularly with regard to the wind

effect, which is a pervasive element of ecological systems and has a wide variety of effects on intermediate species. Wind patterns can vary, and its speed varies correspondingly [5,6]. From recent studies, it is seen that wind affects predation efficiency in various ways. It can change a species' sensing ability in the presence of a predator [7,8]. It may hamper the inherent movement of some species by creating disturbances in surrounding areas. In an experiment, Klimczuk et al. [9] showed that aerial predators may more easily spot reed warbler nests that are exposed by the wind. A higher rate of predation may occur if the victim is less able to detect approaching predators [10]. According to Cherry and Barton's research [11], high wind speed in windy conditions forces prey animals to become more vigilant because wind is found to negatively impact the detection abilities of prey species. Depending on the sort of prey species being pursued, wind can have a variety of effects on how one predator preys on its prey species [12]. For example, according to Stander and Albon [10], under windy conditions, lions (Panthera leo) preyed more frequently on springbok (Antidorcas marsupialis) and zebra (Equus quagga) than on wildebeest (Connochaetes taurinus). According to the previous studies, windy conditions can have a significant impact on species' interactions by altering the mobility of some species [13]. A predator's movement can be hindered, slowed down, and decreased by wind [14,15]. Small-bodied invertebrate aerial predators, such as mosquitoes and flies, have decreased predation success when there is windy weather [16,17]. In contrast, strong winds are advantageous to large predatory birds because they improve their efficacy and mobility. Strong winds also improve their ability to fly, allowing them to spend more time successfully foraging [18,19]. According to Barton's research [20], a windy environment decreases lady beetle hunting effectiveness, which has a detrimental effect on the success of their aphid predation. All of the aforementioned arguments imply that the concept of wind should be introduced into the model system at the time of creating a mathematical model to estimate the dynamics of a predator–prey system. In this context, Barman et al. [21] were the first ones to design a mathematical model by modifying the Holling type-II functional response under windy situations and studying the impacts of it on system dynamics. Later, Barman et al. [22] performed another study in a spatio–temporal modelling sense to predict possible complex dynamics by considering herd behaviour of prey species in windy conditions.

On the other hand, ecology has a seasonal component. The values of parameters of an ecosystem change with the advancement of time. As a result, the dynamics of an ecological system are greatly affected. Therefore, both theoretical and experimental ecologists have performed studies on ecological systems that are vulnerable to seasonal changes. The inherent characteristics of environmental and seasonal perturbations have also been considered in this investigation [23]. Understanding the connection between the size of seasonal fluctuation and system complexity is the fundamental issue. Much research [24–27] has been conducted to examine how the seasons affect the internal biological cycles of simple prey–predator ecosystems. These investigations have demonstrated that these interactions can lead to a variety of spectacular outcomes, including multiple attractors and chaos [28]. So it is important to take into account seasonal variation into the mathematical model.

Numerous natural systems such as weather and climate exhibit chaotic behaviour. With the use of a nonlinear mathematical model, we can analyse this phenomenon. For example, a natural food chain model exhibits chaos according to Hastings and Powell [29]. It becomes difficult to keep chaos under control or to stabilise chaotic population dynamics. A chaotic system can be controlled by small adjustments to the system parameters or initial conditions. In this context, the Hastings and Powell model [29] has been explored by other researchers [30–33], who also took into account some biological aspects, such as alternate food, Allee effects, refuge, diseases, and fear, to control the chaotic dynamics. This article primarily focuses on the control of chaotic dynamics of a model system taken from the article [23] by varying a crucial parameter (which has been newly introduced) in a systematic way. Apart from this, the possible impact on the survival and the huge decline in biomass of the species of that parameter have been further investigated.

On the other hand, the basic idea underpinning evolutionary trade-offs is that improving one characteristic's fitness (or function) must come at the price of lowering that of another one [34]. Life history trade-offs are a type of evolutionary trade-off that are defined as the reduction in fitness (basically, lifetime reproductive success) brought on by one life history feature in exchange for an improvement in fitness brought on by a different life history trait [35]. Life history features, such as those related to growth rate, size of the body, response to stress, timing of reproduction, progeny quantity/quality, life expectancy, and dispersion, are intimately connected to fitness [36]. The trade-off between the amount of energy spent on reproduction and survival is a well-known example. If an organism only has a certain quantity of energy to distribute among all the tasks it must carry out, then the more energy is dedicated to reproduction (increased sexual activity/larger reproductive organs), the less is left for survival (longevity/weapon size). For instance, researchers were able to see that in male fruit flies (Drosophila melanogaster), an increase in reproductive activity is associated with a decrease in lifespan through experimental manipulation in the lab [37]. Research on pinnipeds provides more evidence of the trade-off between reproduction and survival, showing that both genital length and testicular mass are adversely correlated with investment in precopulatory weapons [38]. In general, researchers have presented a predator–prey interaction model and studied it. Here, we have taken general classes of two models—(i) prey–specialist predator model [39] and (ii) prey–generalist predator model [40]—covering the entire class of predator–prey interactions in nature and then studied the effect of seasonality (which is the reality of the environment). We have perturbed both model systems and studied the effects. In this article, it will be interesting to explore whether wind speed has any trade-off relation or not.

This article is divided into different sections that together complete the research findings. Section 2 deals with the formulation of the model systems. The model system's well-posedness is covered in Section 3, while Section 4 examines the model system's overall stability near various equilibrium points. In Section 5, the parametric conditions of global stability are discussed. Extensive numerical simulations are performed in Section 6. Finally, the obtained findings are interpreted in Section 7.

2. Model Formulation

Here, we have considered two different types of predator–prey models; one is for the specialist predator, and the other one is for the generalist predator [41]. Additionally, we have considered the corresponding perturbed version of the proposed model system.

2.1. Model System 1

Here, we have considered a specialist predator–prey model from Upadhyay and Iyengar [23] and modified it by implementing the concept that wind reduces the predation efficiency. The modification of the functional response has been done according to the derivation of Barman et al. [21]. The functional response has been modified by considering the fact that wind speed increases the prey-handling time of predators. They have considered the prey-handling time as

$$\psi(W) \times \text{original prey handling time considering no wind speed,}$$

where the predation efficiency

$$\psi(W) = 1 + \frac{W}{1+W}$$

is based on the following assumptions:

(i) $\psi(0) = 1$; i.e., considering no wind speed, the handling time remains the same as before.

(ii) $\psi'(W) > 0$; i.e., considering wind speed and with the acceleration of this speed, the handling time for each prey per predator continuously increases.

However, to get detailed insight of the modification of this functional response, the readers are referred to study the article [21]. In this way, the following predator–prey model has been formulated:

$$\begin{cases} \dfrac{dX}{dt} = AX\left(1-\dfrac{X}{K}\right) - \dfrac{C_1XY}{1+W+B_1X+\frac{B_1WX}{1+W}}, \\ \dfrac{dY}{dt} = -CY + \dfrac{C_2XY}{1+W+B_2X+\frac{B_2WX}{1+W}}, \end{cases} \tag{1}$$

with starting conditions

$$X(0) = X_0 > 0,\ Y(0) = Y_0 > 0, \tag{2}$$

where A, K, C_1, W, B_1, C, C_2, B_2 are all positive parameters. Here, A denotes the intrinsic growth rate of prey species, K is the environmental carrying capacity of the prey species, C_1 represents the maximum consumption rate of prey species, W indicates the level of wind speed in the proposed system, C is the natural mortality rate of the specialist predator species, C_2 stands for the food conversion rate from prey to predator species, and B_1^{-1}, B_2^{-1} are the half-saturation constants considering no wind speed. Here, we have taken $B_1 = B_2$. The units of all the parameters are provided in Table 1.

Table 1. Units of all non-negative parameters of System (1).

Parameter	Unit
X	(prey density)
Y	(predator density)
A	$(\text{time})^{-1}$
K	(prey density)
C_1	$(\text{predator density})^{-1}$
C_2	$(\text{prey density})^{-1}$
$B_1 = B_2$	$(\text{prey density})^{-1}$
C	$(\text{time})^{-1}$
W	$(\text{time})^{-1}$

2.2. Model System 2

Similarly, the following model has been considered by taking the predator as a generalist; that means these types of predators have some common prey with the specialist predators [40]. The growth of these predators happens according to the Leslie–Gower scheme. However, the model considering wind speed can be presented as follows:

$$\begin{cases} \dfrac{dX}{dt} = AX\left(1-\dfrac{X}{K}\right) - \dfrac{C_1XY}{1+W+B_1X+\frac{B_1WX}{1+W}} - \dfrac{C_3X^2}{X^2+D_1^2}, \\ \dfrac{dY}{dt} = C_4Y - \dfrac{C_5Y^2}{X}, \end{cases} \tag{3}$$

with starting conditions

$$X(0) = X_0 > 0,\ Y(0) = Y_0 > 0. \tag{4}$$

The units of all the parameters are provided in Table 2.

Remark 1. *Here, the term* $\dfrac{C_3X^2}{X^2+D_1^2}$ *is incorporated in the system to consider the impact of grazing pressure of the generalist predators on specialist predators as they share some common food resources. It is assumed that at high population densities, the consumption of prey species of generalist predators becomes asymptotic, and hence, the sigmoid type of functional response has been*

considered here. Interested readers can read the article by Upadhyay and Iyengar [23] and [39,40] for better understanding related to the formulation of the model and the ecological descriptions of every parameter considering no wind speed.

Table 2. Units of all other non-negative parameters of System (3).

Variable/Parameter	Unit
C_3	(prey density)·(time)$^{-1}$
D_1	(prey density)
C_4	(time)$^{-1}$
C_5	(predator density)$^{-1}$·(prey density)·time^{-1}

Note: The units of the other parameters are the same as those of System (1) described in Table 1.

2.3. Perturbed Model System 1

In this subsection, we have considered the perturbed version of System (1) by adding the sinusoidal term $\epsilon \sin \theta t$, where ϵ and θ, respectively, denote the strength of oscillation around an average value and angular frequency of the oscillations occurring due to seasonality. Here, the intrinsic growth rate A of prey species and the natural mortality rate C of predator species have been chosen to undergo seasonality. After giving the perturbation, the autonomous system becomes non-autonomous. Here, we have made the non-autonomous system again an autonomous system by increasing its dimension. For this purpose, we have introduced a new variable $\Theta = \theta t$, and the obtained model is shown below:

$$\begin{cases} \dfrac{dX}{dt} = AX\left(1 - \dfrac{X}{K}\right) - \dfrac{C_1XY}{1 + W + B_1X + \frac{B_1WX}{1+W}} + Ag_1(X, \Theta), \\ \dfrac{dY}{dt} = -CY + \dfrac{C_2XY}{1 + W + B_2X + \frac{B_2WX}{1+W}} - Cg_2(Y, \Theta), \\ \dfrac{d\Theta}{dt} = \theta, \end{cases} \tag{5}$$

with starting conditions

$$X(0) = X_0 > 0,\ Y(0) = Y_0 > 0,\ \Theta(0) = \Theta_0 > 0, \tag{6}$$

where

$$\Theta = \theta t,\ g_1(X, \Theta) = \epsilon X \sin \Theta,\ g_2(Y, \Theta) = \epsilon Y \sin \Theta,$$

and $\theta = \frac{2\pi}{t}$, where t represents the time period of sinusoidal oscillations, and $0 < \epsilon \leq 1$.

2.4. Perturbed Model System 2

Similarly, we have considered the perturbed version of System (3) by taking A and C_4 as the seasonality parameters. The resulting system is:

$$\begin{cases} \dfrac{dX}{dt} = AX\left(1 - \dfrac{X}{K}\right) - \dfrac{C_1XY}{1 + W + B_1X + \frac{B_1WX}{1+W}} - \dfrac{C_3X^2}{X^2 + D_1^2} + Ag_1(X, \Theta), \\ \dfrac{dY}{dt} = C_4Y - \dfrac{C_5Y^2}{X} + C_4g_2(Y, \Theta), \\ \dfrac{d\Theta}{dt} = \theta, \end{cases} \tag{7}$$

with starting conditions

$$X(0) = X_0 > 0,\ Y(0) = Y_0 > 0,\ \Theta(0) = \Theta_0 > 0, \tag{8}$$

where

$$\Theta = \theta t,\ g_1(X,\Theta) = \epsilon X \sin\Theta,\ g_2(Y,\Theta) = \epsilon Y \sin\Theta.$$

3. Model Validation

3.1. Positivity

Theorem 1. *Every solution of both Model Systems* (1) *and* (3) *with respect to respective initial conditions exists in* $[0,\infty)$ *and remains positive* $\forall\ t > 0$.

Proof. The proof is trivial and so omitted. □

3.2. Boundedness

Theorem 2. *Every solution of both Model Systems* (1) *and* (3) *with respect to the respective initial conditions is always bounded.*

Proof. The proof is trivial and so omitted. □

Remark 2. *The checking of positivity and boundedness of a proposed system is necessarily required because no population can be negative and/or unbounded due to limited food resources.*

3.3. Persistence

Definition 1. *Let* $q_1,\ q_2,\ Q_1,\ Q_2$ *be positive constants and be independent of the initial conditions* $X(0) > 0,\ Y(0) > 0$ *of System* (1). *If the underlying restrictions hold,*

$$q_1 \le \lim_{t\to\infty} inf\ X(t) \le \lim_{t\to\infty} sup\ X(t) \le Q_1,$$
$$q_2 \le \lim_{t\to\infty} inf\ Y(t) \le \lim_{t\to\infty} sup\ Y(t) \le Q_2,$$

then System (1) *will be called a 'permanent system'.*

Lemma 1. *Let* $\xi,\ \chi,\ X(0) > 0$. *Now, if* $\frac{dX}{dt} \le X(t)\Big(\xi - \chi X(t)\Big)$, *then* $\lim_{t\to\infty} \sup X(t) \le \frac{\xi}{\chi}$. *Also, if* $\frac{dX}{dt} \ge X(t)\Big(\xi - \chi X(t)\Big)$, *then* $\lim_{t\to\infty} \inf X(t) \ge \frac{\xi}{\chi}$.

Theorem 3. *System* (1) *becomes permanent if the two requirements listed below are true at the same time:*

(i) $1 + W > KL_2$;

(ii) $e_2(L_3 - \epsilon_3) > e_1(2 + W + \frac{W}{1+W})$.

Proof. The first equation of Model System (1) gives us

$$\frac{dX}{dt} \le X(1 - X). \tag{9}$$

By using Lemma 1 in (9), we can derive

$$\lim_{t\to\infty} \sup X(t) \le 1. \tag{10}$$

Therefore, for an arbitrary small $\epsilon_1 > 0$, $\exists$ a positive number $T_1 > 0$ such that

$$X(t) \le 1 + \epsilon_1, \quad \forall t \ge T_1.$$

Now,

$$\frac{d}{dt}\left(X+\frac{1}{e_2}Y\right) \leq (1+e_1)X - e_1\left(X+\frac{1}{e_2}Y\right).$$

$$\text{i.e.,} \quad \frac{d}{dt}\left(X+\frac{1}{e_2}Y\right) + e_1\left(X+\frac{1}{e_2}Y\right) \leq L_1, \text{where } L_1 = (1+e_1)(1+\epsilon_1).$$

In this way, we can write

$$\limsup_{t\to\infty}\left(X+\frac{c_1}{c_2}Y(t)\right) \leq \frac{L_1}{e_1}.$$

As a result, we can say that there is a positive real number L_2 for which $\limsup_{t\to\infty} Y(t) \leq L_2$. So we will be able to discover another sufficiently small value for $\epsilon_2 > 0$ for which $\exists$ a positive real number $T_2 > T_1$ such that $Y(t) \leq L_2 + \epsilon_2, \ \forall \ t \geq T_2$. Hence, the system is always dissipative.

From first equation of (1), we get

$$\frac{dX}{dt} \geq X\left\{\left(1-\frac{L_2}{W+1}\right) - X\right\}. \tag{11}$$

So on the basis of Lemma 1, we may obtain

$$\liminf_{t\to\infty} X(t) \geq L_3, \quad \text{where } L_3 = \frac{1+W-KL_2}{1+W}$$

provided $1+W > KL_2$.
Thus, for any arbitrary small $\epsilon_3 > 0$, $\exists$ a positive number $T_3 > T_2$ such that

$$X(t) \geq L_3 - \epsilon_3, \quad \forall \ t \geq T_3.$$

Now, from the second equation of Model System (1), we achieve

$$\frac{dY}{dt} \geq Y(A' - B'Y), \quad \text{where } A' = \frac{e_2(L_3-\epsilon_3) - e_1(2+W+\frac{W}{1+W})}{1+W+X+\frac{WX}{1+W}} \text{ and } B' = \frac{1}{1+W+X+\frac{WX}{1+W}}.$$

Now, using Lemma 1, we get

$$\liminf_{t\to\infty} Y(t) \geq \frac{A'}{B'}$$

provided $e_2(L_3-\epsilon_3) > e_1(2+W+\frac{W}{1+W})$.

Let us choose $\epsilon = \min\left\{L_3, \frac{A'}{B'}\right\}$. Then for $\epsilon > 0$, $\liminf_{t\to\infty} X(t) \geq \epsilon$ and $\liminf_{t\to\infty} Y(t) \geq \epsilon$. Therefore, if the aforementioned requirements are true, System (1) is uniformly persistent. □

Remark 3. *From the above theorem, it is observed that System (1) is inextricably dependent on the strength of the wind speed parameter for the survival of all the species in a feasible region.*

Remark 4. *In a similar way, we can show that the dynamical System (3) will be permanent for* $1 > \frac{e_1}{e_2(1+W)} + \frac{1}{p_1^2}$. *Here also, the populations stay in the domain/region based on the strength of the wind parameter.*

4. General Stability Analysis and Hopf Bifurcation of the Model Systems

4.1. Equilibria, Their Conditions of Existence, and Local Stability Analysis of System (1)

At first, we reduced the number of parameters of System (1) by setting a proper choice of non-dimensional variables as follows:

$$x = \frac{X}{K},\ y = \frac{C_1}{A}Y, T = At,\ C = A, B_1 = B_2 = \frac{1}{K},\ e_1 = \frac{C}{A},\ e_2 = \frac{KC_2}{A}.$$

So System (1) becomes

$$\begin{cases} \dfrac{dx}{dT} = x(1-x) - \dfrac{xy}{1+W+x+\frac{Wx}{1+W}}, \\ \dfrac{dy}{dT} = -e_1 y + \dfrac{e_2 xy}{1+W+x+\frac{Wx}{1+W}}, \end{cases} \tag{12}$$

with initial conditions

$$x(0) = x_0 > 0,\ y(0) = y_0 > 0. \tag{13}$$

To check the local stability, first of all, we must derive the Jacobian matrix. For this cause, let us now consider the right-hand side of Model System (12) as a set of distinct functions as shown below:

$$f(x,y) = x(1-x) - \frac{xy}{1+W+x+\frac{Wx}{1+W}},$$
$$g(x,y) = -e_1 y + \frac{e_2 xy}{1+W+x+\frac{Wx}{1+W}}.$$

The Jacobian matrix can be written as

$$J(x,y) = \begin{pmatrix} J_{11} & J_{12} \\ J_{21} & J_{22} \end{pmatrix},$$

where

$$J_{11} = \frac{\partial f}{\partial x} = 1 - 2x - \frac{(1+W)y}{\left(1+W+x+\frac{Wx}{1+W}\right)^2},$$
$$J_{12} = \frac{\partial f}{\partial y} = -\frac{x}{1+W+x+\frac{Wx}{1+W}},$$
$$J_{21} = \frac{\partial g}{\partial x} = \frac{e_2(1+W)y}{\left(1+W+x+\frac{Wx}{1+W}\right)^2},$$
$$J_{22} = \frac{\partial g}{\partial y} = \frac{e_2 x}{1+W+x+\frac{Wx}{1+W}} - e_1.$$

Now, let us analyse the existence of equilibrium points along with their local stability for Model System (12) one-by-one in the following way.

Theorem 4. *The equilibrium point $E_0(0,0)$ is known as a trivial equilibrium point, and it always persists. Model System (12) always exhibits locally unstable phenomenon around the point $E_0(0,0)$ at any time T.*

Proof. $\lambda_1 = 1\ (> 0)$ and $\lambda_2 = -e_1\ (< 0)$ are the eigenvalues of the Jacobian matrix obtained at the trivial equilibrium point $E_0(0,0)$. As a result, since $E_0(0,0)$ is a saddle point, it exhibits unstable behaviour there. □

Theorem 5. *The equilibrium point $E_1(1,0)$ is known as the axial or predator-free equilibrium point, and it always persists. Model System (12) exhibits locally asymptotically stable phenomenon around the predator-free equilibrium point $E_1(1,0)$ at any time T for $e_2 < e_1\left(2 + W + \frac{W}{1+W}\right)$, i.e., the ratio of the parameter e_2 and e_1 should be smaller than the expression containing the wind parameter.*

Proof. The eigenvalues of the Jacobian matrix computed at $E_1(1,0)$ are $\lambda_1 = -1\ (< 0)$ and $\lambda_2 = -e_1 + \frac{e_2}{2+W+\frac{W}{1+W}}$. So the system will show stable phenomenon around $E_1(1,0)$ for $e_2 < e_1\left(2 + W + \frac{W}{1+W}\right)$. □

Remark 5. *The system may experience a bifurcation at $e_2 = e_1\left(2 + W + \frac{W}{1+W}\right)$.*

Theorem 6. *The interior or co-existence equilibrium point $E^*(x^*, y^*)$ of System (12) exists for $e_2 > e_1\left(2 + W + \frac{W}{1+W}\right)$. The system shows locally asymptotically stable (LAS) behaviour around this interior equilibrium point $E^*(x^*, y^*)$ for*

$$1 - 2x^* - \frac{e_1(1+W)(1-x^*)}{e_2 x^*} < 0.$$

Proof. The interior or co-existence equilibrium point $E^*(x^*, y^*)$ is where

$$x^* = \frac{e_1(1+W)}{e_2 - e_1 - \frac{e_1 W}{1+W}}, \tag{14}$$

$$y^* = \frac{e_2(1+W)\left(e_2 - e_1(1+W) - e_1 - \frac{e_1 W}{1+W}\right)}{\left(e_2 - e_1 - \frac{e_1 W}{1+W}\right)^2}. \tag{15}$$

Now, both the expressions x^* and y^* become positive under the following restrictions:

$$e_2 > e_1(1+W) + e_1 + \frac{e_1 W}{1+W}. \tag{16}$$

So $e_2 > e_1(2 + W + \frac{W}{1+W})$ is the foremost condition behind the subsistence of the interior steady state $E^*(x^*, y^*)$.

The characteristic equation of the Jacobian matrix associated with the interior steady state $E^*(x^*, y^*)$ is

$$\lambda^2 - (J_{11}^* + J_{22}^*)\lambda + J_{11}^* J_{22}^* - J_{12}^* J_{21}^* = 0, \tag{17}$$

where J_{11}^*, J_{12}^*, J_{21}^*, J_{22}^* are obtained by evaluating J_{11}, J_{12}, J_{21}, J_{22} at interior steady state $E^*(x^*, y^*)$.

Now,

$$\text{Trace}(J(x^*, y^*)) = J_{11}^* + J_{22}^* = 1 - 2x^* - \frac{e_1(1+W)(1-x^*)}{e_2 x^*},$$

$$\det(J(x^*, y^*)) = J_{11}^* J_{22}^* - J_{12}^* J_{21}^* = \frac{e_2(1+W)x^* y^*}{\left(1 + W + x^* + \frac{W x^*}{1+W}\right)^3}\ (> 0).$$

Equation (17) will have two negative real roots for $J_{11}^* + J_{22}^* < 0$, i.e., for

$$1 - 2x^* - \frac{e_1(1+W)(1-x^*)}{e_2 x^*} < 0.$$

Hence, we have the theorem. □

Theorem 7. *The existence condition* $e_2 > e_1\left(2 + W + \frac{W}{1+W}\right)$ *of the interior equilibrium point* $E^*(x^*, y^*)$ *and the local stability condition* $1 - 2x^* - \frac{e_1(1+W)(1-x^*)}{e_2 x^*} < 0$ *depends on the wind parameter. Thus, it crucially controls the behaviour (existence, survival, etc. of the species) of the interior point.*

4.2. Hopf Bifurcation Analysis

For $1 - 2x^* - \frac{e_1(1+W)(1-x^*)}{e_2 x^*} = 0$, Equation (17) possesses two purely imaginary roots; and Equation (17) becomes:

$$\lambda^2 + \frac{e_2(1+W)x^*y^*}{\left(1 + W + x^* + \frac{Wx^*}{1+W}\right)^3} = 0. \tag{18}$$

So we have obtained two purely imaginary eigenvalues such as $\lambda_{1,2} = \pm i\omega_0$, where

$$\omega_0 = \sqrt{\frac{e_2(1+W)x^*y^*}{\left(1 + W + x^* + \frac{Wx^*}{1+W}\right)^3}}.$$

Now, the task is to prove the transversality condition, i.e., the non-zero speed of the eigenvalues for crossing the imaginary axis. This can be accomplished by checking the expression of the derivative of the $J_{11}^* + J_{22}^*$ with respect to wind speed W as a non-zero quantity.

At this time,

$$\frac{d(J_{11}^* + J_{22}^*)}{dW} = -\frac{e_1}{K}\left(1 + \frac{1+W}{Kx^{*2}}\right)\frac{e_2 - e_1 - \frac{e_1 W}{1+W} + \frac{e_1}{1+W}}{\left(e_2 - e_1 - \frac{e_1 W}{1+W}\right)^2} - \frac{e_1 K(1-x^*)}{e_2 x^*} \neq 0.$$

As a result, System (12) exhibits Hopf bifurcation close to the interior steady state $E^*(x^*, y^*)$ with respect to wind speed W.

4.3. Equilibria, Their Conditions of Existence, and Local Stability Analysis of System (3)

At first, we reduced the number of parameters of System (3) by setting the proper choice of non-dimensional variables as follows:

$$x = \frac{X}{K},\ y = \frac{C_1}{A}Y, T = At,\ C_3 = AK, B_1 = \frac{1}{K},\ e_1 = \frac{C_4}{A},\ e_2 = \frac{C_5}{KC_1},\ P_1 = \frac{D_1}{K}.$$

So System (3) becomes

$$\begin{cases} \frac{dx}{dT} = x(1-x) - \frac{xy}{1 + W + x + \frac{Wx}{1+W}} - \frac{x^2}{x^2 + P_1^2}, \\ \frac{dy}{dT} = e_1 y - \frac{e_2 y^2}{x}, \end{cases} \tag{19}$$

with initial conditions

$$x(0) = x_0 > 0,\ y(0) = y_0 > 0. \tag{20}$$

Here, the Jacobian matrix is given by

$$J(x,y) = \begin{pmatrix} 1-2x-\dfrac{(1+W)y}{\left(1+W+x+\frac{Wx}{1+W}\right)^2}+\dfrac{2P_1^2x}{(x^2+P_1^2)^2} & -\dfrac{x}{1+W+x+\frac{Wx}{1+W}}, \\ \dfrac{e_2y^2}{x^2} & e_1-\dfrac{2e_2y}{x} \end{pmatrix}.$$

Let us now state Model System (12)'s equilibria existence criteria along with their local stability requirement, expressed by the following theorems surrounding each equilibrium point.

Theorem 8. *The trivial equilibrium point $E_0(0,0)$ always exists, and it is unstable at any moment T.*

Proof. $\lambda_1 = 1$ and $\lambda_2 = e_1$ (> 0) are the eigenvalues of the Jacobian matrix calculated at $(0,0)$, which results in the trivial point $E_0(0,0)$ as being unstable. □

Theorem 9. *The axial or predator-free equilibrium point $E_1(x_1,0)$ always exists, and it is always unstable.*

Proof. The axial or predator-free equilibrium point is $E_1(x_1,0)$, where x_1 can be obtained from the following equation:

$$x_1{}^3 - x_1{}^2 + (1+P_1^2)x_1 - P_1^2 = 0. \tag{21}$$

Equation (21) always possesses at least one positive root. Now, $\lambda_1 = 1 - 2x_1 + \frac{2x_1P_1^2}{(x_1^2+P_1^2)^2}$ and $\lambda_2 = e_1$ are the eigenvalues of the Jacobian matrix calculated at $(x_1,0)$. So $E_1(x_1,0)$ will always be unstable. □

Theorem 10. *The interior steady state $E^*(x^*,y^*)$ shows stability or instability depending upon various parametric restrictions.*

Proof. The interior steady state is $E^*(x^*,y^*)$, where

$$y^* = \frac{e_1x^*}{e_2}, \tag{22}$$

and x^* can be obtained from the following equation:

$$R_1x^{*4} + R_2x^{*3} + R_3x^{*2} + R_4x^* + R_5 = 0, \tag{23}$$

where

$$\begin{aligned} R_1 &= e_2\left(1+\frac{W}{1+W}\right), \\ R_2 &= e_1 - e_2\left(\frac{W}{1+W} - W\right), \\ R_3 &= e_2P_1^2\left(1+\frac{W}{1+W}\right) - e_2(1+W), \\ R_4 &= e_1P_1^2 + e_2 + \frac{e_2W}{1+W} - e_2P_1^2\left(\frac{W}{1+W} - W\right), \\ R_5 &= e_2(1+W)(1-P_1). \end{aligned}$$

Now, the interior steady state $E^*(x^*, y^*)$ will exist depending upon the existence of a positive root of Equation (23).

The local stability analysis of the interior steady state $E^*(x^*, y^*)$ has been done in the Numerical Simulation section because it is very complicated to analyse analytically. Similarly, the existence of Hopf bifurcation analysis has also been performed numerically. □

5. Global Stability Analysis

5.1. For System (12)

Theorem 11. *If the following stipulation is true, the interior steady state $E^*(x^*, y^*)$ of System (12) becomes globally asymptotically stable:*

$$\left(2 + W + \frac{W}{1+W}\right)\left(1 + W + x^* + \frac{Wx^*}{1+W}\right) > \left(1 + \frac{W}{1+W}\right)y^*.$$

Proof. Let us take the Lyapunov function in the underlying manner:

$$L(x, y) = \alpha_1 \int_{x^*}^{x} \frac{x - x^*}{x} dx + \alpha_2 \int_{y^*}^{y} \frac{y - y^*}{y} dy,$$

where α_1 and α_2 are defined as positive constants and are chosen appropriately.

Now, performing differentiation on the aforementioned function with respect to T, we get

$$\begin{aligned}
\frac{dL}{dT} &= \alpha_1 \frac{x - x^*}{x}\frac{dx}{dT} + \alpha_2 \frac{y - y^*}{y}\frac{dy}{dT}, \\
&= \alpha_1 (x - x^*)\left\{1 - x - \frac{y}{1 + W + x + \frac{Wx}{1+W}}\right\} + \alpha_2 \left\{-e_1 + \frac{e_2 x}{1 + W + x + \frac{Wx}{1+W}}\right\}, \\
&= -\alpha_1 (x - x^*)^2 \left\{1 - \frac{\left(1 + \frac{W}{1+W}\right)y^*}{\left(1 + W + x + \frac{Wx}{1+W}\right)\left(1 + W + x^* + \frac{Wx^*}{1+W}\right)}\right\} - \\
&\frac{\alpha_1 (x - x^*)(y - y^*)}{\left(1 + W + x + \frac{Wx}{1+W}\right)\left(1 + W + x^* + \frac{Wx^*}{1+W}\right)}\left[-\alpha_2 e_2 (1 + W) + 1 + W + x^* + \frac{Wx^*}{1+W}\right].
\end{aligned}$$

Now, we choose $\alpha_2 = \frac{1+W+x^*+\frac{Wx^*}{1+W}}{e_2(1+W)}$. So the above time derivative becomes

$$\begin{aligned}
\frac{dL}{dT} &= -\alpha_1 (x - x^*)^2 \left\{1 - \frac{\left(1 + \frac{W}{1+W}\right)y^*}{\left(1 + W + x + \frac{Wx}{1+W}\right)\left(1 + W + x^* + \frac{Wx^*}{1+W}\right)}\right\}, \\
&< -\alpha_1 (x - x^*)^2 \left\{1 - \frac{\left(1 + \frac{W}{1+W}\right)y^*}{\left(2 + W + \frac{W}{1+W}\right)\left(1 + W + x^* + \frac{Wx^*}{1+W}\right)}\right\}, \qquad (24)
\end{aligned}$$

Now, if the parametric limitation $\left(2 + W + \frac{W}{1+W}\right)\left(1 + W + x^* + \frac{Wx^*}{1+W}\right) > \left(1 + \frac{W}{1+W}\right)y^*$ is applied, then from (24), we can obtain

$$\frac{dL}{dT} < 0.$$

Therefore, according to the invariance principle of Lyapunov–Lassalle [42], the steady state $E^*(x^*, y^*)$ becomes asymptotically stable globally if the aforementioned condition holds true. □

5.2. For System (19)

Theorem 12. *The dynamical System (19) will be globally asymptotically stable around its interior equilibrium point for*

(i) $\frac{\left(1+\frac{W}{1+W}\right)y^*}{l\left[1+W+\left(1+\frac{W}{1+W}\right)x^*\right]}+\frac{l+x^*}{(1+P_1^2)(x^{*2}+P_1^2)}<1,$

(ii) $e_2>e_1l,$

where $l=1-\frac{e_1}{e_2(1+W)}-\frac{1}{P_1^2}.$

Proof. The proof can be done in a similar fashion. □

Remark 6. *The parametric restrictions obtained for both Systems (12) and (19) are sufficient conditions. As with the earlier case, they depend on the wind parameter, which reveals the fact that the stability of both systems may depend on the wind parameter.*

6. Numerical Simulations

In this section, we have performed extensive numerical simulation to explore the model systems' possible dynamics. For this purpose, we have used MATLAB (R2018a) software. We have mainly used the 'Ode45' toolbox and default error tolerance level for the simulations. Since we want to explore the effect of wind speed on the dynamics of all four systems, we have considered all the parameter values from the article [23] and varied the levels of wind speed accordingly. The adopted parameter sets for different model systems can be seen from Table 3. Now, let us explore the systems' possible dynamics individually in the following subsections.

Table 3. Parameter set for different model systems (∗ = assumed).

Model System	Parameter Values	Source
System 1	$A=2,\ K=40,\ B_1=0.1,\ B_2=0.1,\ C_1=0.1,\ C_2=0.2,\ C=1,\ W=*$	[23]
System 2	$A=2,\ K=100,\ B_1=0.1,\ C_1=0.1,\ C_3=1,\ W=*,\ D_1=10,\ C_4=0.45,\ C_5=0.2$	[23]
Perturbed System 1	$A=2,\ K=75,\ B_1=0.1,\ B_2=0.1,\ C_1=0.1,\ C_2=0.2,\ C=1, \theta=0.681,\ \epsilon=0.6,\ W=*$	[23]
Perturbed System 2	$A=2,\ K=100,\ B_1=0.1,\ C_1=0.1,\ C_3=1,\ W=*,\ D_1=10,\ C_4=0.45,\ C_5=0.2, \theta=0.153,\ \epsilon=0.6$	[23]

6.1. For System (1)

To start with, we have plotted the phase portrait dynamics both in the absence and presence of wind speed for System (1). The system shows unstable behaviour by producing limit-cycle oscillation considering no wind speed, i.e., for $W=0$, as shown in Figure 1a. But considering wind speed, i.e., for $W=0.4$, the limit-cycle oscillation vanishes and the system becomes stable, as portrayed in Figure 1b. The possible ecological reason behind this scenario might be the overpredation of prey species considering no wind speed. But considering a certain wind speed threshold, the predator individuals may not be able to catch the prey species conveniently, which gives a space for the prey species to grow and maintains balance in the prey–predator interactions.

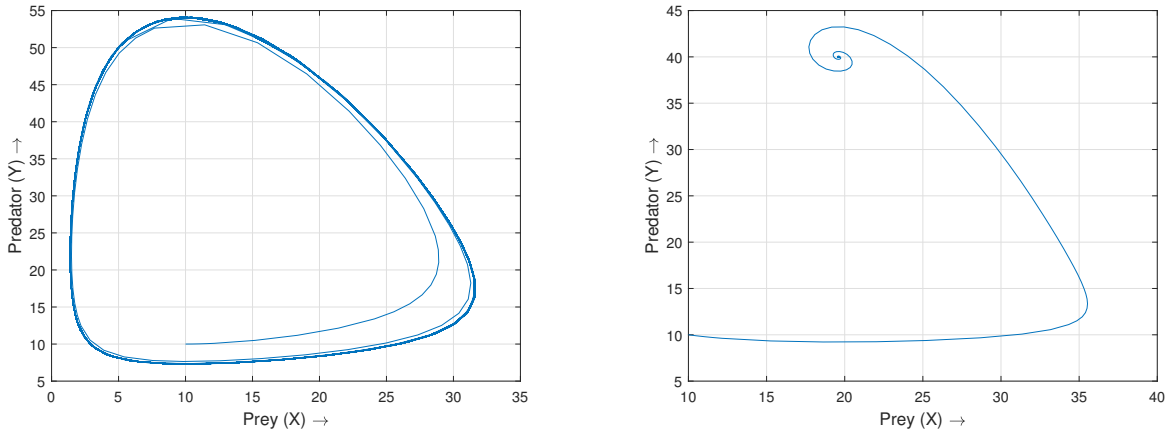

(**a**) $W = 0$ (**b**) $W = 0.4$

Figure 1. Phase portrait plot for different levels of wind speed for System (1). Subfigure (**a**) and Subfigure (**b**), respectively, represent the unstable and stable behaviour of the corresponding system. The parameter values are taken from Table 3.

In Figure 2, we have plotted the Hopf bifurcation diagram with respect to the wind speed for $[0, 0.5]$. Here, it is seen that the system remains stable until it crosses the threshold value $W = W^* = 0.25$. Both the prey and predator population densities oscillate between some ranges when the wind level lies below the aforesaid threshold value. As soon as it crosses the corresponding threshold value, the oscillation of the species stops, and the system becomes stable. However, to know the effect of wind speed on population density, we plotted the biomass of both the species in the range $W \in [0.2, 1.5]$ in Figure 3. From Figure 3a, it is seen that the density of the prey population increases with the rise in wind speed and then saturates after reaching a particular wind speed threshold value. On the other hand, the predator biomass starts to decline with the rise in wind speed and eventually goes very close to zero.

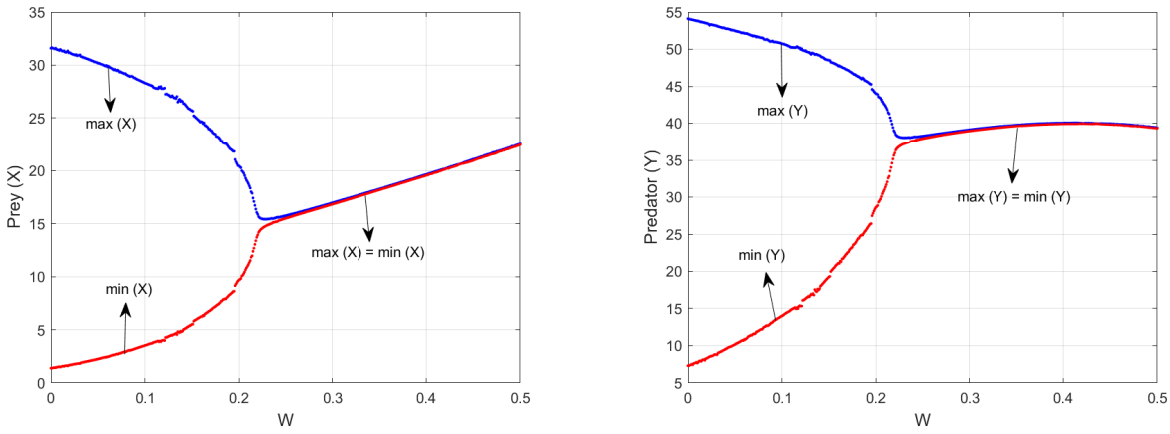

(**a**) (**b**)

Figure 2. Plot of Hopf bifurcation diagram with respect to wind speed W for Model System (1) for $W \in [0, 0.5]$. The other parameter values have been taken from Table 3.

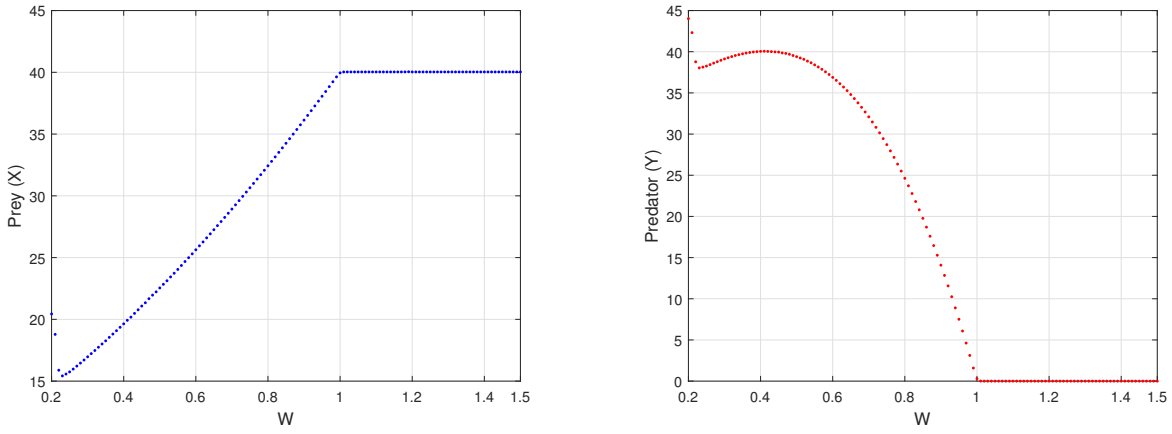

(**a**) (**b**)

Figure 3. Plot of population biomass with respect to wind speed W for Model System (1) for $W \in [0.2, 1.5]$. The other parameter values have been taken from Table 3.

Remark 7. *The ecological reason behind the huge decline in biomass of the specialist predator can be interpreted as follows:*

The specialist predator entirely relies upon the availability of a favourable prey species for its livelihood, so it becomes very tough for it to survive without the proper interactions with prey species. Since wind speed acts as an obstacle for it and reduces the predation efficiency, for higher values of wind level, the predation efficiency starts to reduce, which eventually causes the declination of its biomass. Once the level of the wind speed crosses some threshold, the predator species biomass goes very close to zero, and on the other hand, the prey species biomass increases continuously.

6.2. For System (5)

In this subsection, we have considered the perturbed model (5) associated with model (1). Here, we have considered the perturbation on the parameters A and C, respectively, as in the article [23]. Our main aim is to determine the impact of wind speed W on the perturbed system dynamics considering the parameter set described in Table 3. So in Figure 4, we have plotted the phase portrait and time-series plot considering no wind speed for the system. From Figure 4, it is noticed that System (5) shows chaotic behaviour around the interior steady state. But for $W = 1.5$, it is seen that this chaotic attractor turns into a simple periodic oscillations as exhibited in Figure 5. So it can be said that the level of the wind speed crucially impacts the system dynamics and is responsible for controlling the chaotic behaviour of the considered system. Again, to check the further impact of the wind parameter on both population biomasses, we have considered an increased level of wind speed $W = 2$ and noticed that the predator population biomass goes very close to zero, while the prey biomass sustains a range in an oscillatory manner. This observation has been depicted in Figure 6. The possible ecological explanation behind this scenario is very much apparent.

The bifurcation diagram for the perturbed System (5) with respect to the wind speed W has been depicted in Figure 7. From Figure 7a, it is noticed that the system undergoes chaotic oscillation considering no wind speed; but considering wind speed (for increasing the value of it), the system undergoes a simple periodic oscillation between the range 0 to 120. However, for the increasing value of the wind parameter, the predator population goes very close to zero. The threshold that accounts for the huge decline in biomass of the predator species is $W = 1.57$, below which the system shows multi-periodic oscillation.

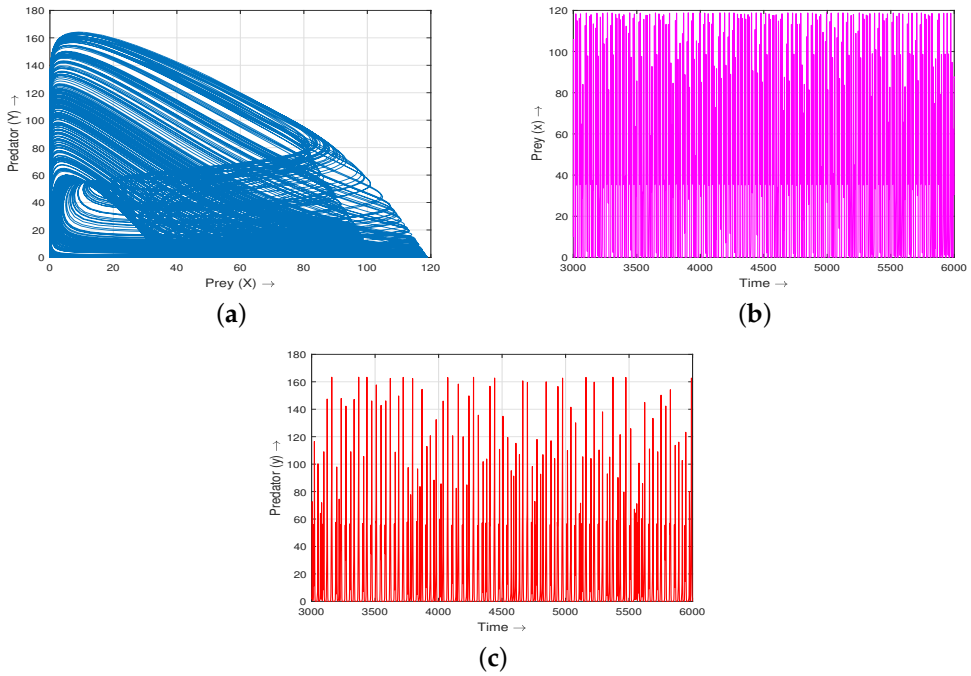

Figure 4. Considering no wind speed, the perturbed System (5) exhibits chaotic behaviour: (**a**) displays the phase plane projection of chaotic attractor, while (**b**,**c**) show the corresponding time-series solution of prey and predator species, respectively. The parameter set has been used from Table 3.

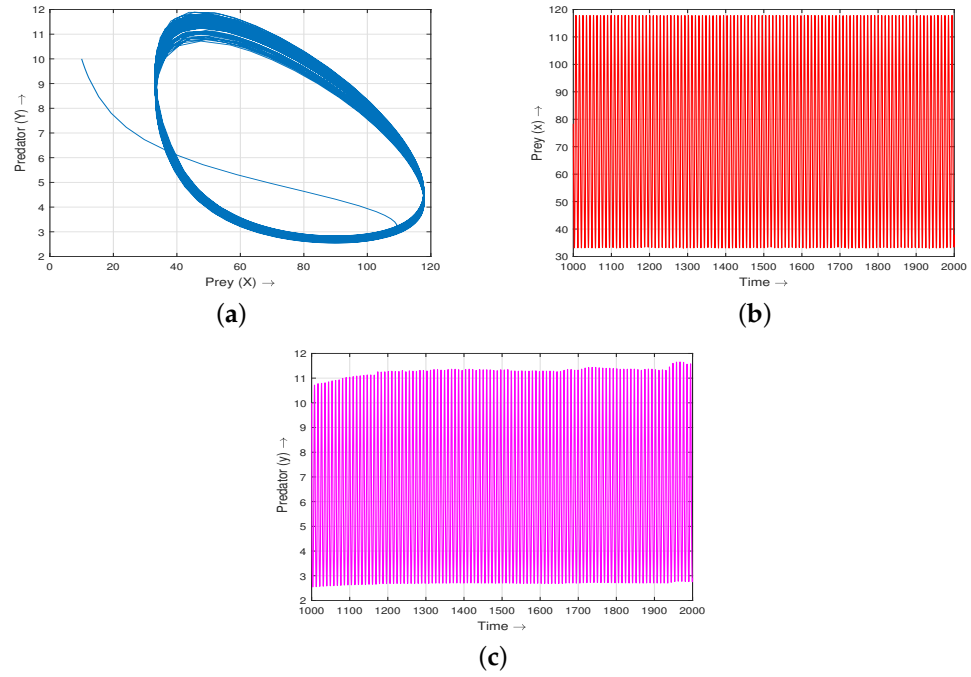

Figure 5. Plot of phase portraits and time evolution for prey species considering wind speed $W = 1.5$ for the perturbed System (5). Here, the chaotic attractor disappears considering wind speed. The other parameter values have been taken from Table 3.

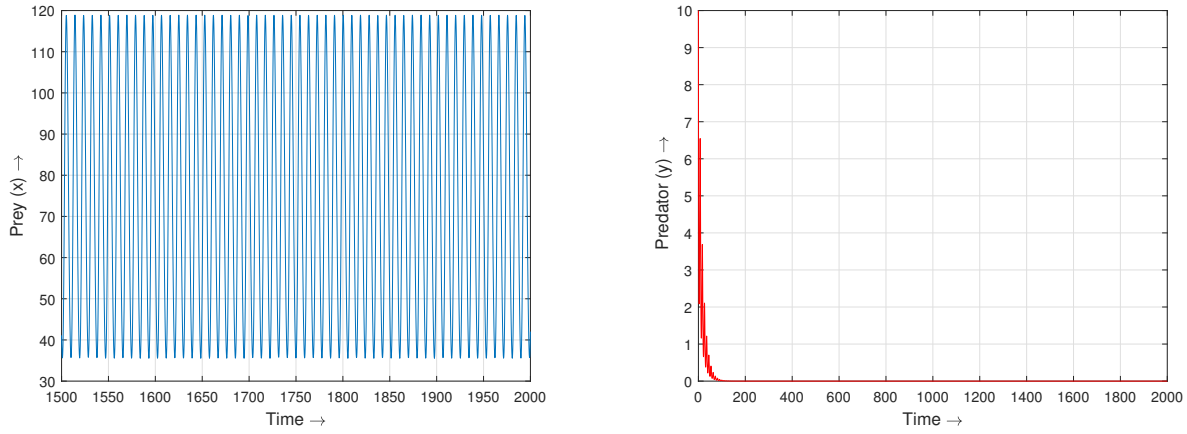

(**a**) (**b**)

Figure 6. Time-series plot for $W = 2$ for the perturbed System (5). It shows that for a higher level of wind speed, the prey population oscillates in a particular region while the predator population goes very close to zero. The other parameter values have been taken from Table 3.

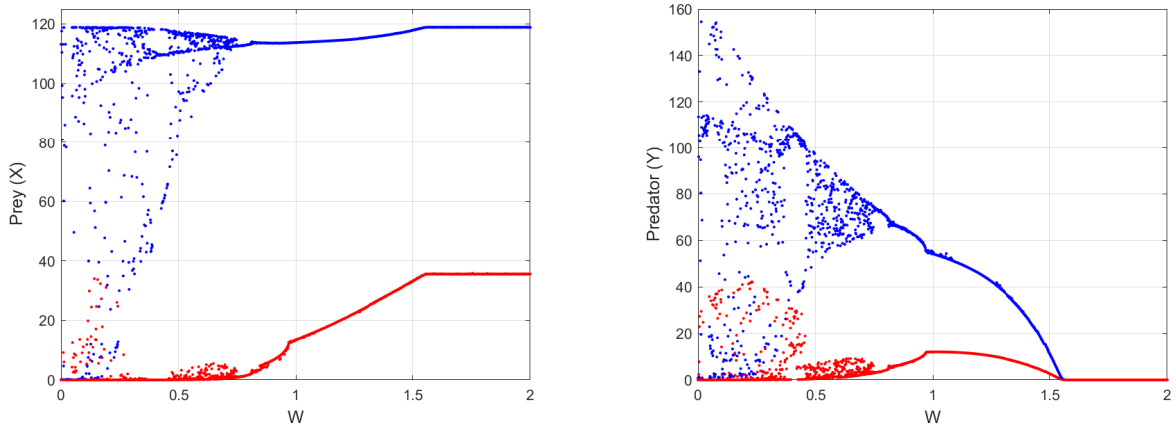

(**a**) (**b**)

Figure 7. Plot of bifurcation diagram with respect to the wind speed W for System (5). It exhibits that the prey population oscillates, while the predator population goes very close to zero with the rise in wind parameter value. The other parameter values have been taken from Table 3.

Remark 8. ***Reason behind the occurrence of chaos and its mitigation:***

Considering no wind speed, the system exhibits a chaotic phenomenon (see the article [23]). There may be many possible reasons behind this scenario. One possible reason can be interpreted as a continuous fluctuation in the population biomass in an unpredictable way. This continuous fluctuation in the population biomass may occur depending upon over-predation of prey species or something related to the interacting relationships among them. Considering wind speed, this unpredictable periodic fluctuation in the biomass turns to a simple periodic fluctuation within a feasible range; that means wind speed can control the randomness of population biomass fluctuations in a meaningful way. It is thought that wind speed controls this chaotic behaviour by regaining a proper balance for the interactions among the prey species and the specialist predator species.

In Figure 8, we plotted the dynamics of the Lyapunov exponents both in the presence and the absence of wind speed for System (5). From Figure 8a, we noticed that the prey population exhibits chaotic phenomenon as the Lyapunov exponent takes the non-negative value; but the predator species does not exhibit chaotic phenomenon, as it is seen that the corresponding Lyapunov exponent is always negative. However, in the presence of wind

speed, i.e., for $W = 1.5$, both of the Lyapunov exponents of the species take negative values (as shown in Figure 8b), which eventually expresses the non-chaotic phenomenon of the interacting species.

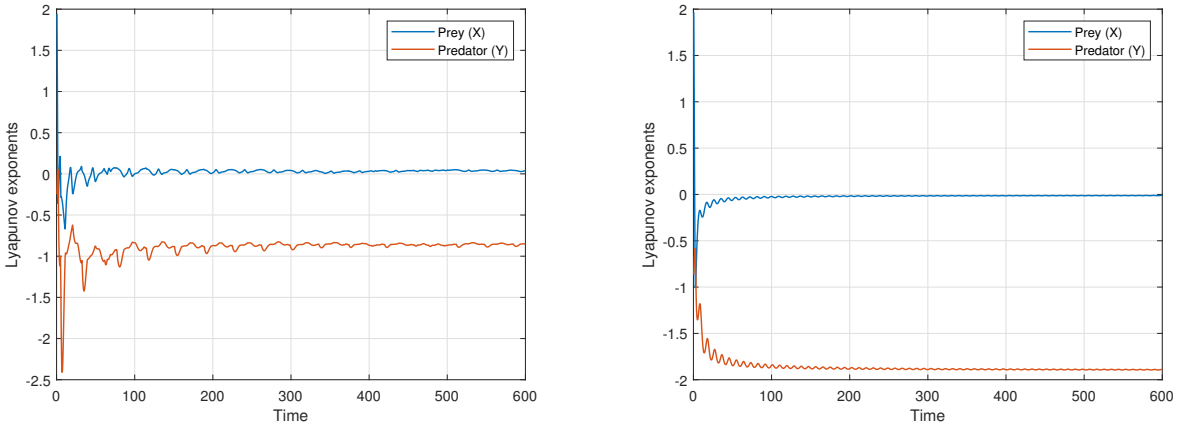

(**a**) For $W = 0$ (**b**) For $W = 1.5$

Figure 8. Plot of Lyapunov exponents with respect to the wind speed W for System (5). It exhibits that the prey population shows chaotic behaviour while the predator population shows non-chaotic behaviour. The other parameter values have been taken from Table 3.

6.3. For System (3)

Here, initially, we have plotted the phase portrait dynamics both in the absence and presence of wind speed for System (3). The system shows unstable behaviour by producing limit-cycle oscillation considering no wind speed, i.e., for $W = 0$, as shown in Figure 9a. The corresponding time-series plot has been shown in Figure 9b. But considering wind speed, i.e., for $W = 0.5$, the limit-cycle oscillation vanishes, and the system becomes stable, as portrayed in Figure 10a. The corresponding time-series plot has been shown in Figure 10b. The possible ecological reason behind this scenario might be the over-predation of prey species considering no wind speed. But considering a certain amount of wind speed threshold value, the predator populations may not be able to catch the prey species conveniently, which gives space for the prey species to grow and maintains a balance in the prey–predator interactions.

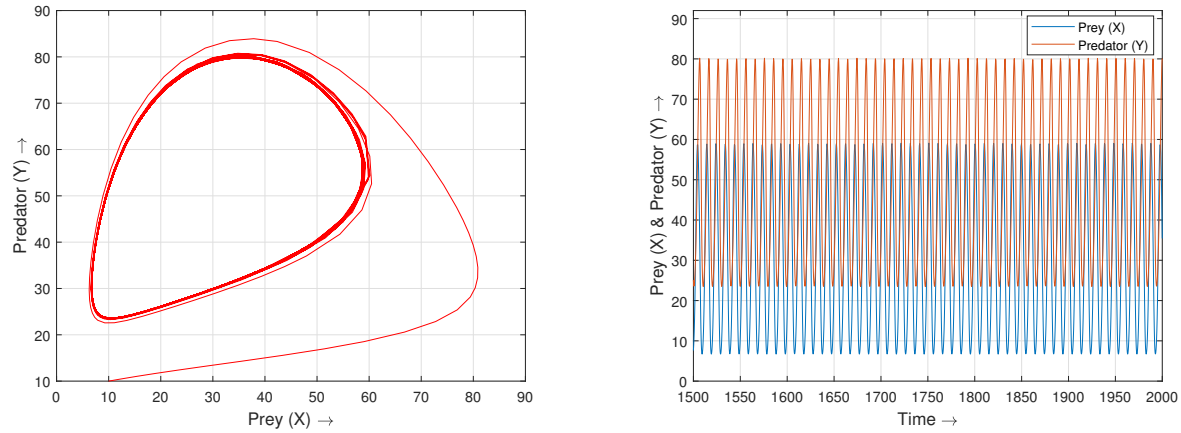

(**a**) (**b**)

Figure 9. Plot of phase portraits and time evolution for prey species considering no wind speed for System (3). The other parameter values have been taken from Table 3.

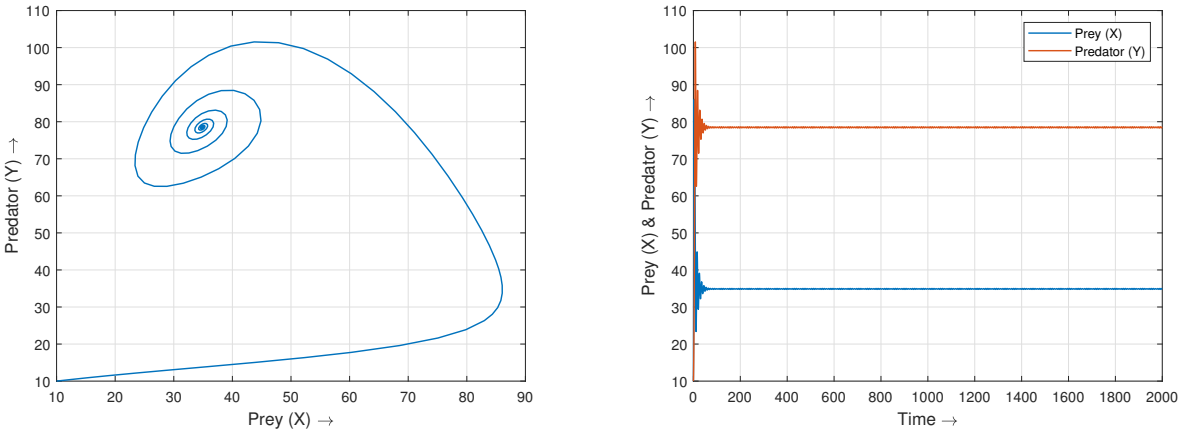

Figure 10. Plot of phase portraits and time evolution for prey species considering wind speed ($W = 0.5$) for System (3). The other parameter values have been taken from Table 3.

In Figure 11, we plotted the Hopf bifurcation diagram with respect to the wind speed for $[0, 0.5]$. Here, it is seen that the system remains stable until it crosses the threshold value $W = W^* = 0.35$. Both the prey and predator population densities oscillates between some ranges when the wind level lies below the mentioned threshold value. As soon as it crosses the corresponding threshold value, the oscillation of the species stops, and the system becomes stable.

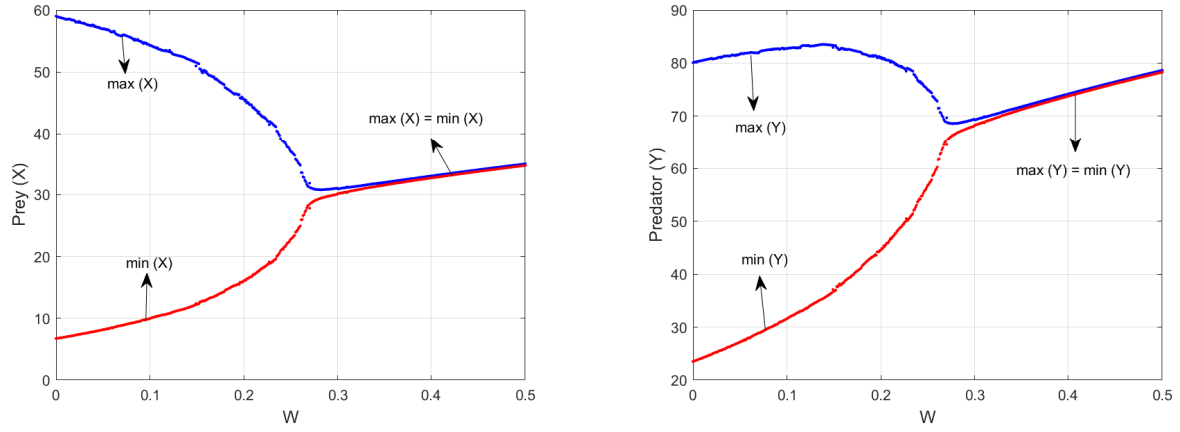

Figure 11. Plot of Hopf bifurcation diagram with respect to wind speed W for Model System (3) for $W \in [0, 0.5]$. The other parameter values have been taken from Table 3.

Remark 9. *Considering no wind speed, the generalist predator exhibits periodic fluctuation; but considering wind speed, it shows stable behaviour. Unlike the specialist predator, here, the generalist predator can persist without the presence of the prey species because it has other food options. Considering no wind speed, the generalist predator over-predates its favourite food and creates an imbalance on the biotic relationships, which thus demonstrates the periodic fluctuation of its biomass. As opposed to that, considering wind speed, this imbalance is overcame, and as a result, the systems exhibit stable behaviour around the co-existence steady state.*

The population biomass plot for both species is shown in Figure 12 with respect to the wind parameter W for System (3). It has been noted that both populations grow more biomass as the wind parameter value increases.

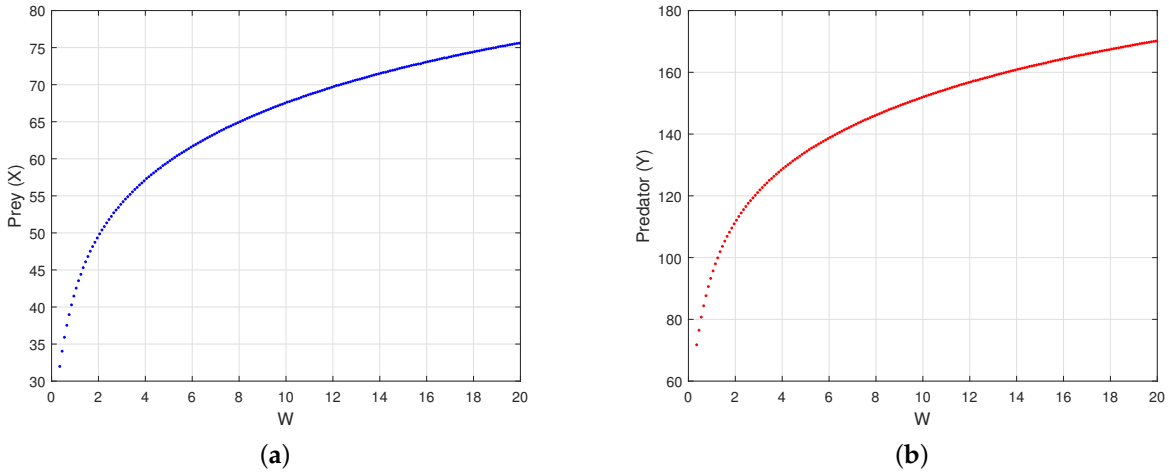

(**a**) (**b**)

Figure 12. Plot of population density with respect to wind speed W for Model System (3) for $W \in [0.35, 20]$. The other parameter values have been taken from Table 3.

6.4. For System (7)

In this subsection, we have considered the perturbed Model (7) associated with Model (3). Here, we have considered the perturbation of the parameters A and C_4, respectively, as in the article [23]. Our main aim is to determine the impact of wind speed W on the perturbed system dynamics considering the parameter set described in Table 3. So in Figure 13, we have plotted the phase portrait and time-series plot considering no wind speed for the system. Figure 4 shows that System (5) experiences period-four oscillating behaviour around the interior steady state. But for $W = 8$, it is seen that this period-four oscillating behaviour turns into a simple periodic oscillation as exhibited in Figure 14. So it can be said that the level of the wind speed crucially impacts the system dynamics and is responsible for controlling the period-four oscillating behaviour of the considered system.

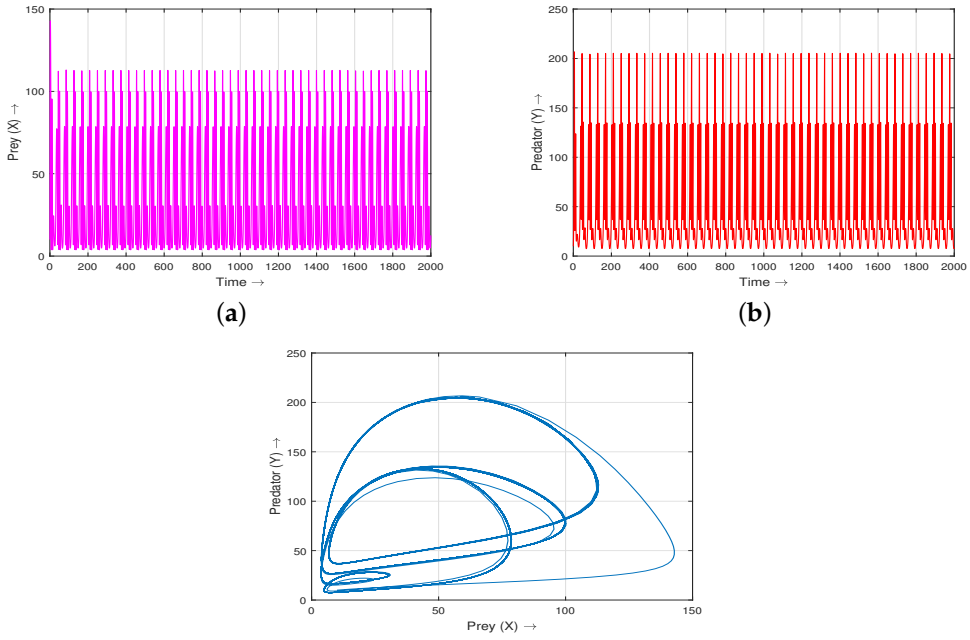

(**a**) (**b**)

(**c**)

Figure 13. Time-series and phase portrait plot of the perturbed System (7) considering no wind, which reveals the system undergoes period-four oscillations. The other parameter values have been taken from Table 3.

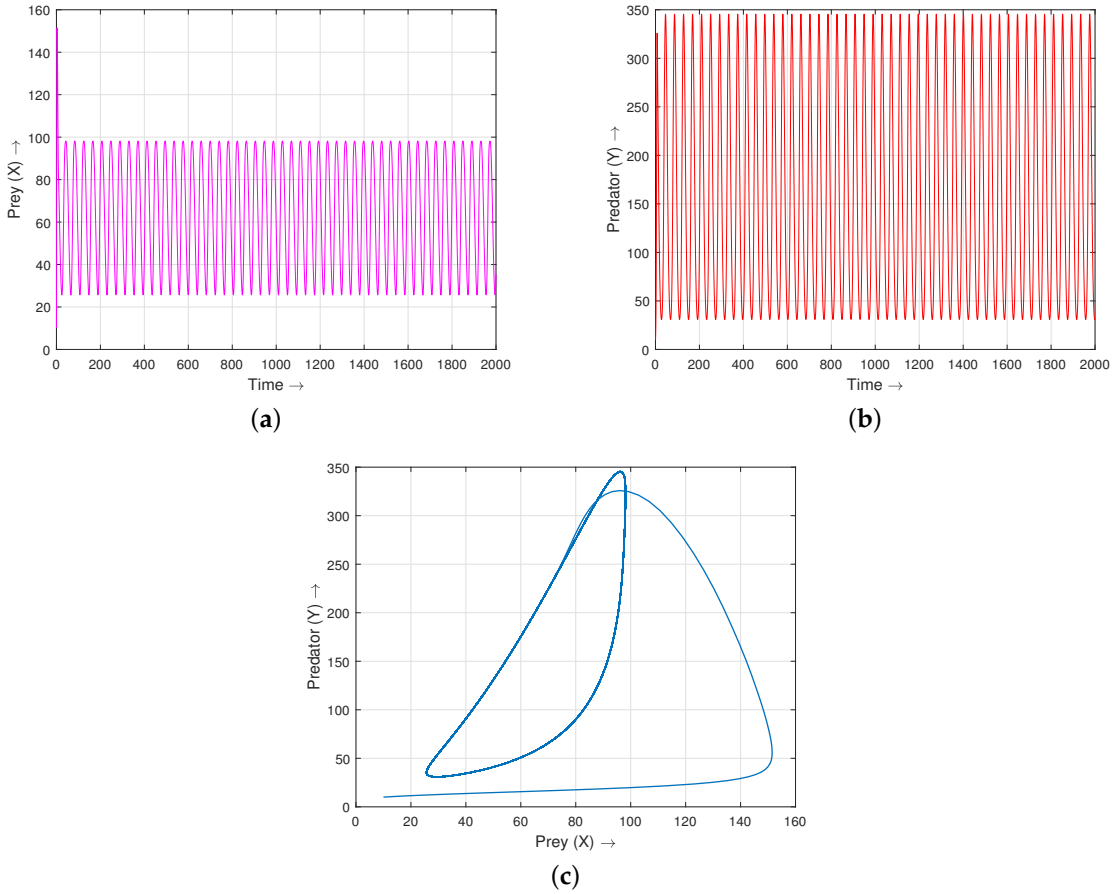

Figure 14. Time-series and phase portrait plot of the perturbed System (7) considering wind, $W = 8$, which reveals the system undergoes simple periodic oscillations. The other parameter values have been taken from Table 3.

Remark 10. ***Reason behind the occurrence of period-4 oscillation and its control:***

Considering no wind speed, the system exhibits period-4 oscillation. There may be many possible reasons behind this scenario. One possible reason can be interpreted as a continuous fluctuation in the population biomass in a feasible range in a periodic way. This fluctuations in the population biomass may occur depending upon over-predation of prey species or something related to the interacting relationships among them. Considering wind speed, this period-4 oscillation in the biomass turns to a simple periodic fluctuation within a feasible range; that means wind can control the period-4 oscillation in the population biomass fluctuation in a meaningful way. It is thought that wind controls this scenario by regaining a proper balance for the interactions among the prey species and the generalist predator species.

Figure 15a clearly exhibits that for $W = 0.5$, $\epsilon = 0.6$, System (5) exhibits chaotic nature. However, this chaotic nature can be transformed into period-2 oscillation if the strength of the seasonality parameter ϵ is increased by fixing the wind speed parameter value at $W = 0.5$ (see Figure 15b). On the other hand, fixing the strength of the seasonality parameter ϵ at $\epsilon = 0.6$, the chaotic phenomenon can be completely transformed into a simple periodic oscillation as exhibited in Figure 15c. From this contradictory behaviour of these parameters with each other in the context of the stability, we can say that there is a trade-off between these two parameters.

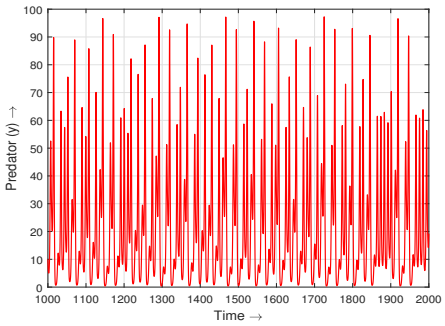

(**a**) $W = 0.5$, $\epsilon = 0.6$

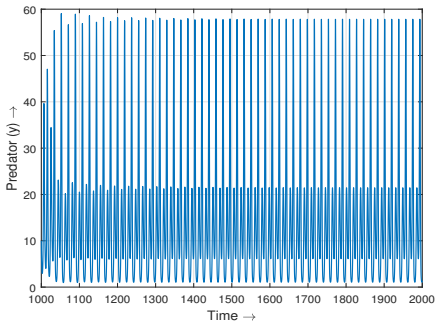

(**b**) $W = 0.5$, $\epsilon = 0.9$

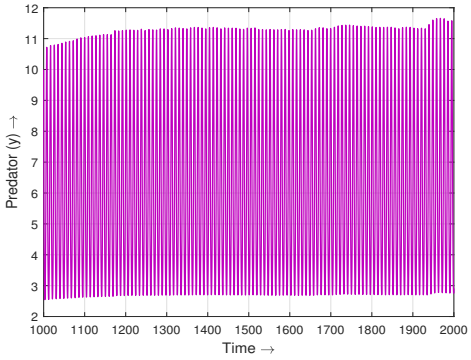

(**c**) $W = 1.5$, $\epsilon = 0.6$

Figure 15. Time-series plot of the perturbed System (5) considering different combinations between the wind speed W and strength of seasonality ϵ. The other parameter values have been taken from Table 3.

Remark 11. *The study of predator–prey models based on wind effect was lacking significantly as compared to other models due to the insufficient amount of experimental evidence. However, in the article [11], the authors have beautifully summarized all the information regarding the interactions of species related to wind speed. All the presented information dealt with some limited types of species. However, in this article, we have considered broader types of interactions between prey species and specialist as well as generalist predators. We have modified the models presented in the article [23] with the wind factor, and the obtained results vary significantly from those published previously. The previous results have shown that the perturbed version of a prey–specialist predator system undergoes chaotic behaviour, whereas we have shown that this chaos can be controlled with the help of the wind parameter. On the other hand, for the perturbed version of a prey–generalist predator system, it is observed that wind can transform the period-4 oscillation (which was not presented in that article) into a simple limit-cycle oscillation. For the non-perturbed version of a prey–specialist predator system, the wind parameter acts as a stabilizing factor, which matches the results of the article [21].*

6.5. For Perturbed System 1

Let us consider another form (considered in article [43]) of the perturbed version of System (1) as follows:

$$\begin{cases} \dfrac{dX}{dt} = A(t)X\left(1 - \dfrac{X}{K}\right) - \dfrac{C_1XY}{1 + W + B_1X + \frac{B_1WX}{1+W}}, \\ \dfrac{dY}{dt} = -C(t)Y + \dfrac{C_2XY}{1 + W + B_2X + \frac{B_2WX}{1+W}}, \end{cases} \tag{25}$$

with starting conditions

$$X(0) = X_0 > 0,\ Y(0) = Y_0 > 0, \tag{26}$$

where $A(t) = A + A_1 \sin \theta t$, $C(t) = C + C_{11} \sin \theta t$, $0 < A_1 < A$, $0 < C_{11} < C$.

Here, we have considered the parameter set as $A = 2$, $K = 40$, $C_1 = 0.1$, $C_2 = 0.2$, $B_1 = 0.1$, $B_2 = 0.2$, $C = 1$, $\theta = \frac{2\pi}{365}$, $A_1 = 0.5$, $C_{11} = 0.4$. The perturbed System (25) has been plotted for different time series by varying the wind speed parameter W. From Figure 16a, it is seen that in the absence of wind speed, the system undergoes a bursting pattern (for details, please see the article [43]); this pattern continues for $W = 0.5$ also, as shown in Figure 16b. However, for $W = 1.5$, this pattern vanishes, and there exist very few individuals of the predator species (Figure 16c).

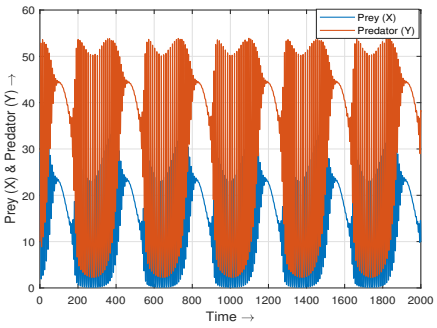

(**a**) $W = 0$

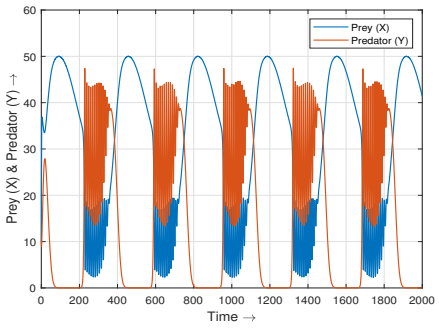

(**b**) $W = 0.5$

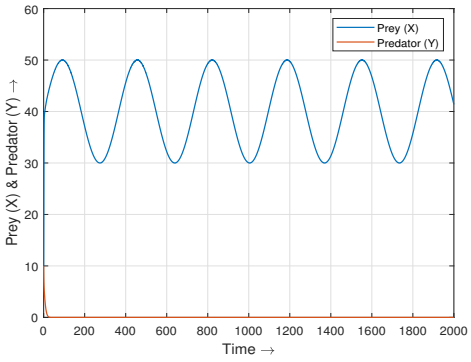

(**c**) $W = 1.5$

Figure 16. Time-series plot of the perturbed System (25) considering different values of the wind speed parameter W. The other parameter values have been mentioned in the text.

6.6. For Perturbed System 2

Let us consider another form (considered in the article [43]) of the perturbed version of System (3):

$$\begin{cases} \dfrac{dX}{dt} = A(t)X\left(1 - \dfrac{X}{K}\right) - \dfrac{C_1XY}{1 + W + B_1X + \frac{B_1WX}{1+W}} - \dfrac{C_3X^2}{X^2 + D_1^2}, \\ \dfrac{dY}{dt} = C_4(t)Y - \dfrac{C_5Y^2}{X}, \end{cases} \tag{27}$$

with starting conditions

$$X(0) = X_0 > 0,\ Y(0) = Y_0 > 0,\ \Theta(0) = \Theta_0 > 0, \tag{28}$$

where $A(t) = A + A_1 \sin \theta t$, $C_4(t) = C_4 + C_{41} \sin \theta t$, $0 < A_1 < A$, $0 < C_{41} < C_4$.

Here, we have considered the parameter set as $A = 2$, $K = 100$, $C_1 = 0.1, C_3 = 1, B_1 = 0.1$, $D_1 = 10$, $C_4 = 0.45$, $C_{41} = 0.4$, $C_5 = 0.2$, $\theta = \frac{2\pi}{365}$, $A_1 = 0.5$ The perturbed System (27) is plotted as different time series by varying the wind speed parameter W. From Figure 17a, it is seen that in the absence of wind speed, the system undergoes a bursting pattern (for details, please see the article [43]); this pattern continues for $W = 0.5$ also, as shown in Figure 17b. However, for $W = 1.5$, this pattern vanishes, as depicted in Figure 16c.

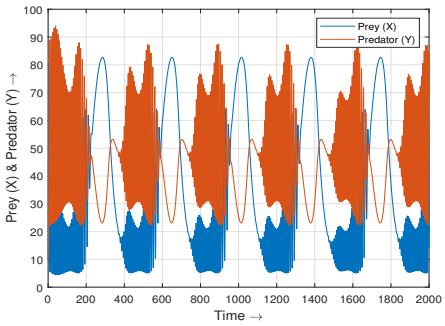

(**a**) $W = 0$

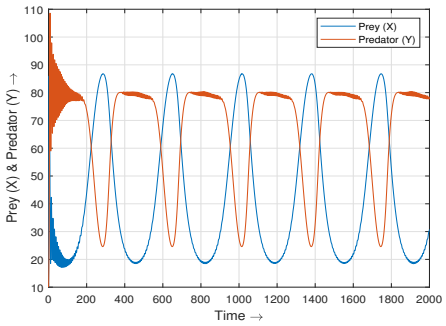

(**b**) $W = 0.5$

.

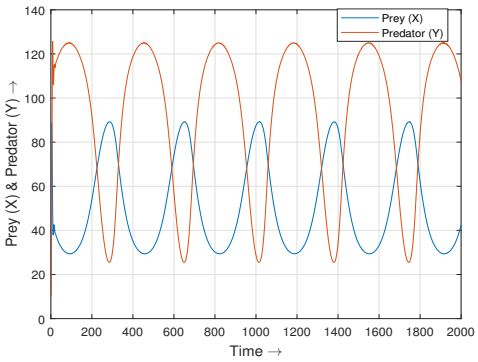

(**c**) $W = 1.5$

Figure 17. Time-series plot of the perturbed System (27) considering different values of the wind speed parameter W. The other parameter values have been mentioned in the text.

Remark 12. *For System (5), in the absence of the wind speed parameter, we have obtained the chaotic phenomenon; whereas for System (25), we have obtained the bursting pattern. For higher values of wind speed, the predator population goes very close to zero for the earlier perturbed system; here also, it goes very close to zero. For System (7), in the absence of the wind speed parameter, we have obtained period-4 oscillations; whereas for System (27), we have obtained the bursting pattern. For higher values of wind speed, the populations simply oscillate for both of these two perturbed versions.*

7. Conclusions and Discussion

In this article, two continuous predator–prey models and their corresponding perturbed versions have been considered and studied in windy conditions. The models and the parameters that are considered for seasonal perturbation have been considered from the article [23]. It is noticed that the speed level of the wind parameter has a significant impact on controlling the systems' stability. When the predator is considered a specialist, it is observed that the wind parameter stabilizes the non-perturbed system through the occurrence of a Hopf bifurcation. However, considering no wind speed, the corresponding perturbed version shows chaotic behaviour, which can be controlled by the varying level of wind speed. Considering wind speed, the chaotic attractor turns to a simple limit-cycle oscillation; thus, wind can control the occurrence of such a chaotic attractor. Moreover, for higher levels of wind speed, the non-perturbed system experiences a huge decline in

the biomass of the predator species. On the other hand, when the predator is considered as a generalist, it is observed that the wind parameter stabilizes the non-perturbed system through the occurrence of a Hopf bifurcation in a similar way to the case of the specialist predator. But here, considering no wind speed, the corresponding perturbed version shows period-4 oscillation, which can be controlled by the varying level of wind speed. Considering wind speed, the period-4 orbit turns to a simple limit-cycle oscillation; thus, wind can control the occurrence of such complex dynamics. So it is seen that wind has a great impact on the system dynamics of all the model systems. In this article, all the models are formulated based on the fact that the predator reduces its hunting rate due to the obstacle created by the wind speed. However, more research can be performed in view of the increased predation rate of the predator species in the context of windy conditions.

Author Contributions: D.B.: Conceptualization, Formal analysis, Investigation, Software, Writing—original draft. R.K.U.: Conceptualization, Investigation, Methodology, Project administration, Supervision, Writing—review and editing. All authors have read and agreed to the published version of the manuscript.

Funding: This research received no external funding.

Data Availability Statement: Data are contained within the article.

Conflicts of Interest: The authors declare no conflict of interest.

References

1. Wang, X.; Zanette, L.; Zou, X. Modelling the fear effect in predator–prey interactions. *J. Math. Biol.* **2016**, *73*, 1179–1204. [CrossRef] [PubMed]
2. Balcı, E. Predation fear and its carry-over effect in a fractional order prey–predator model with prey refuge. *Chaos Solitons Fractals* **2023**, *175*, 114016. [CrossRef]
3. Liang, Z.; Meng, X. Stability and Hopf bifurcation of a multiple delayed predator–prey system with fear effect, prey refuge and Crowley–Martin function. *Chaos Solitons Fractals* **2023**, *175*, 113955. [CrossRef]
4. Hang, L.; Zhang, L.; Wang, X.; Li, H.; Teng, Z. A hybrid predator–prey model with general functional responses under seasonal succession alternating between Gompertz and logistic growth. *Adv. Differ. Equations* **2020**, *2020*, 1–21. [CrossRef]
5. McVicar, T.R.; Roderick, M.L.; Donohue, R.J.; Li, L.T.; Van Niel, T.G.; Thomas, A.; Grieser, J.; Jhajharia, D.; Himri, Y.; Mahowald, N.M.; et al. Global review and synthesis of trends in observed terrestrial near-surface wind speeds: Implications for evaporation. *J. Hydrol.* **2012**, *416*, 182–205. [CrossRef]
6. Vautard, R.; Cattiaux, J.; Yiou, P.; Thépaut, J.N.; Ciais, P. Northern Hemisphere atmospheric stilling partly attributed to an increase in surface roughness. *Nat. Geosci.* **2010**, *3*, 756–761. [CrossRef]
7. Hayes, A.R.; Huntly, N.J. Effects of wind on the behavior and call transmission of pikas (Ochotona princeps). *J. Mammal.* **2005**, *86*, 974–981. [CrossRef]
8. Jakosalem, P.G.C.; Collar, N.J.; Gill, J.A. Habitat selection and conservation status of the endemic Ninox hawk-owl on Cebu, Philippines. *Bird Conserv. Int.* **2013**, *23*, 360–370. [CrossRef]
9. Klimczuk, E.; Halupka, L.; Czyż, B.; Borowiec, M.; Nowakowski, J.J.; Sztwiertnia, H. Factors driving variation in biparental incubation behaviour in the reed warbler Acrocephalus scirpaceus. *Ardea* **2015**, *103*, 51–59. [CrossRef]
10. Stander, P.; Albon, S. Hunting success of lions in a semi-arid environment. In Proceedings of the Symposia of the Zoological Society of London, London, UK, 26–27 November 1993; Volume 65, pp. 127–143.
11. Cherry, M.J.; Barton, B.T. Effects of wind on predator-prey interactions. *Food Webs* **2017**, *13*, 92–97. [CrossRef]
12. Van Soest, P.J. Allometry and ecology of feeding behavior and digestive capacity in herbivores: A review. *Zoo Biol. Publ. Affil. Am. Zoo Aquar. Assoc.* **1996**, *15*, 455–479. [CrossRef]
13. Thomas, A.L.; Taylor, G.K. Animal flight dynamics I. Stability in gliding flight. *J. Theor. Biol.* **2001**, *212*, 399–424. [CrossRef] [PubMed]
14. Law, Y.H.; Sediqi, A. Sticky substance on eggs improves predation success and substrate adhesion in newly hatched Zelus renardii (Hemiptera: Reduviidae) instars. *Ann. Entomol. Soc. Am.* **2010**, *103*, 771–774. [CrossRef]
15. Turner, J.; Vollrath, F.; Hesselberg, T. Wind speed affects prey-catching behaviour in an orb web spider. *Naturwissenschaften* **2011**, *98*, 1063–1067. [CrossRef]
16. Yasuoka, J.; Levins, R. Ecology of vector mosquitoes in Sri Lanka-suggestions for future mosquito control in rice ecosystems. *Southeast Asian J. Trop. Med. Public Health* **2007**, *38*, 646.
17. Calcaterra, L.A.; Porter, S.D.; Briano, J.A. Distribution and abundance of fire ant decapitating flies (Diptera: Phoridae: Pseudacteon) in three regions of southern South America. *Ann. Entomol. Soc. Am.* **2005**, *98*, 85–95. [CrossRef]

18. Gilchrist, H.G.; Gaston, A.J. Effects of murre nest site characteristics and wind conditions on predation by glaucous gulls. *Can. J. Zool.* **1997**, *75*, 518–524. [CrossRef]
19. Gilchrist, H.G.; Gaston, A.J.; Smith, J.N. Wind and prey nest sites as foraging constraints on an avian predator, the glaucous gull. *Ecology* **1998**, *79*, 2403–2414. [CrossRef]
20. Barton, B.T. Reduced wind strengthens top-down control of an insect herbivore. *Ecology* **2014**, *95*, 2375–2381. [CrossRef]
21. Barman, D.; Roy, J.; Alam, S. Impact of wind in the dynamics of prey–predator interactions. *Math. Comput. Simul.* **2022**, *191*, 49–81. [CrossRef]
22. Barman, D.; Kumar, V.; Roy, J.; Alam, S. Modeling wind effect and herd behavior in a predator–prey system with spatiotemporal dynamics. *Eur. Phys. J. Plus* **2022**, *137*, 950. [CrossRef]
23. Upadhyay, R.K.; Iyengar, S. Effect of seasonality on the dynamics of 2 and 3 species prey–predator systems. *Nonlinear Anal. Real World Appl.* **2005**, *6*, 509–530. [CrossRef]
24. Rinaldi, S.; Muratori, S.; Kuznetsov, Y. Multiple attractors, catastrophes and chaos in seasonally perturbed predator-prey communities. *Bull. Math. Biol.* **1993**, *55*, 15–35. [CrossRef]
25. Baek, H. An impulsive two-prey one-predator system with seasonal effects. *Discret. Dyn. Nat. Soc.* **2009**, *2009*, 793732. [CrossRef]
26. Gragnani, A.; Rinaldi, S. A universal bifurcation diagram for seasonally perturbed predator-prey models. *Bull. Math. Biol.* **1995**, *57*, 701–712. [CrossRef]
27. Yu, H.; Zhong, S.; Agarwal, R.P.; Sen, S.K. Effect of seasonality on the dynamical behavior of an ecological system with impulsive control strategy. *J. Frankl. Inst.* **2011**, *348*, 652–670. [CrossRef]
28. Parker, T.S.; Chua, L. *Practical Numerical Algorithms for Chaotic Systems*; Springer Science & Business Media: Berlin/Heidelberg, Germany, 2012.
29. Hastings, A.; Powell, T. Chaos in a three-species food chain. *Ecology* **1991**, *72*, 896–903. [CrossRef]
30. Eisenberg, J.N.; Maszle, D.R. The structural stability of a three-species food chain model. *J. Theor. Biol.* **1995**, *176*, 501–510. [CrossRef]
31. Sahoo, B.; Poria, S. The chaos and control of a food chain model supplying additional food to top-predator. *Chaos, Solitons Fractals* **2014**, *58*, 52–64. [CrossRef]
32. Panday, P.; Pal, N.; Samanta, S.; Chattopadhyay, J. Stability and bifurcation analysis of a three-species food chain model with fear. *Int. J. Bifurc. Chaos* **2018**, *28*, 1850009. [CrossRef]
33. Nath, B.; Kumari, N.; Kumar, V.; Das, K.P. Refugia and Allee effect in prey species stabilize chaos in a tri-trophic food chain model. *Differ. Equations Dyn. Syst.* **2019**, *30*, 631–657. [CrossRef]
34. Ou, Q.; Vannier, J.; Yang, X.; Chen, A.; Mai, H.; Shu, D.; Han, J.; Fu, D.; Wang, R.; Mayer, G. Evolutionary trade-off in reproduction of Cambrian arthropods. *Sci. Adv.* **2020**, *6*, eaaz3376. [CrossRef] [PubMed]
35. Zera, A.J.; Harshman, L.G. The physiology of life history trade-offs in animals. *Annu. Rev. Ecol. Syst.* **2001**, *32*, 95–126. [CrossRef]
36. Lancaster, L.T.; Morrison, G.; Fitt, R.N. Life history trade-offs, the intensity of competition, and coexistence in novel and evolving communities under climate change. *Philos. Trans. R. Soc. B Biol. Sci.* **2017**, *372*, 20160046. [CrossRef] [PubMed]
37. Partridge, L.; Farquhar, M. Sexual activity reduces lifespan of male fruitflies. *Nature* **1981**, *294*, 580–582. [CrossRef]
38. Fitzpatrick, J.L.; Almbro, M.; Gonzalez-Voyer, A.; Kolm, N.; Simmons, L.W. Male contest competition and the coevolution of weaponry and testes in pinnipeds. *Evolution* **2012**, *66*, 3595–3604. [CrossRef] [PubMed]
39. Rosenzweig, M.L.; MacArthur, R.H. Graphical representation and stability conditions of predator-prey interactions. *Am. Nat.* **1963**, *97*, 209–223. [CrossRef]
40. Turchin, P.; Hanski, I. An empirically based model for latitudinal gradient in vole population dynamics. *Am. Nat.* **1997**, *149*, 842–874. [CrossRef]
41. Hanski, I.; Hansson, L.; Henttonen, H. Specialist Predators, Generalist Predators, and the Microtine Rodent Cycle. *J. Anim. Ecol.* **1991**, *60*, 353–367. [CrossRef]
42. La Salle, J.P. *The Stability of Dynamical Systems*; SIAM: Bangkok, Thailand, 1976.
43. Barman, D.; Roy, S.; Tiwari, P.K.; Alam, S. Two-fold impacts of fear in a seasonally forced predator-prey system with Cosner functional response. *J. Biol. Syst.* **2023**, *31*, 517–555. [CrossRef]